Acta Astronautica 180 (2021) 73–84

Contents lists available at ScienceDirect

Acta Astronautica

journal homepage: www.elsevier.com/locate/actaastro

Experimental investigation on the starting and flow regulation characteristics of powder supply system for powder engines

Jiangang Yang [a], Chunbo Hu [a,*], Wei Qiang [b], Jiaming Hu [a], Xu Hu [a], Xiaofei Zhu [a]

[a] Science and Technology on Combustion, Internal Flow and Thermo-Structure Laboratory, Northwestern Polytechnical University, Xi'an, Shaanxi, 710072, PR China

[b] Faculty of Science, Engineering and Technology, Swinburne University of Technology, Hawthron, 3122, Australia

ARTICLE INFO

Keywords:
Powder rocket engine
Flow adjustment
Start-up characteristics
Wavelet analysis
Gas-solid two-phase flow

ABSTRACT

Powder supply system is the key component of powder engines with multiple ignition capability, and thrust modulation function. Similar to the pure gas phase, the gas-solid two-phase flow in powder engines also has a choking phenomenon. The powder pneumatic conveying experiments at choked mode and non-choked mode were carried out to compare their conveying characteristics. In the choked mode (mode A and mode B), when the initial pressure of the fluidization chamber is higher than the pressure in the stable stage, the powder supply system is prone to flow peaks. In the choked mode A where the amount of fluidization gas is determined by the area of the throttle channel, the powder supply system is prone to fluctuations, and the frequency and amplitude of the fluctuation are related to the throttle channel area. The choked mode A has good repeatability and flow regulation performance when the throttle channel area is large. Employing pressure simulator and wavelet analysis, the transition from choked flow to non-choked flow was achieved and the effective frequency (<20 Hz) of the powder supply system is obtained. Experimental results and theoretical analysis show that powder flow has an upper limit in the non-choked mode.

1. Introduction

Powder engine is a kind of new concept engines, which takes high-energy metal powder or non-metal powder (Al, Mg, B) as fuel, and the oxidizer can be solid, liquid or gas materials [1–4]. Similar to liquid engines, the storage of powder fuel in powder engines is isolated from the combustion chamber. During the working process of powder engines, powder fuel is first fluidized and transported from the tank of the powder supply system to the combustion chamber, and then the powder fuel is dispersed and combusted with the oxidant in the combustion chamber. On account of the specificity of powder fuel, the powder engine owns some functions of liquid rocket engine, like multiple-ignition capability and thrust adjustment function. Through different propellant combinations, powder engines can be applied to missile power systems (Al/AP powder rocket engines, powder fuel ramjet engines) [5,6] and Mars exploration (Mg/CO_2 powder rocket engines) [7,8]. Therefore, powder engines have broad application prospects.

In order to fill the gaps left by the output powder and ensure the consistent of the powder stacked state in the storage tank, the powder supply system generally uses a light-weight piston to push the powder. The way to drive the piston is generally divided into motor drive and pneumatic drive [9,10]. When the gas pressure in the powder storage tank is high, the force required to drive the piston is very large. Ordinary motors are difficult to meet the requirements, and there are guide rods in the motor, which is not conducive to the integration of the powder engine system. Therefore, most of the existing engine researches adopt the pneumatic driving piston method. Although the speed of the piston driven by a motor is stable, the fluidization process of the powder in the fluidization chamber is not completely constant. Thus, once the amount of powder provided by the piston is greater than the actual output of the powder storage tank, the system is prone to instability [10]. At present, due to the lack of accurate online direct measurement of powder flow, it is difficult to adjust the speed of the motor in real time with negative feedback to ensure stable powder supply.

Similar to the pure gas phase, a choking phenomenon existing in the gas-solid two-phase flow has been proved by experiments [11,12]. When a gas-powder mixture with a certain stagnation status (i.e. constant pressure and temperature) flows out of a powder supply system through the minimum section of pipe at choking condition, the gas-solid two-phase flow state in the powder storage tank is not affected by the combustion chamber. According to whether the two-phase flow is choked or not at the minimum section of pipe, the powder supplying

* Corresponding author.
E-mail address: huchunbo@nwpu.edu.cn (C. Hu).

https://doi.org/10.1016/j.actaastro.2020.12.004
Received 19 September 2020; Received in revised form 25 November 2020; Accepted 3 December 2020
Available online 9 December 2020

methods can be divided into choked mode and non-choked mode [12]. Obviously, different powder supply methods have great effects on the working characteristics of the powder supply system, such as start-up characteristics and flow adjustment characteristics. There are still some unresolved problems in two powder supply modes, and the influence rules are not yet clear.

For the non-choked powder supply mode, powder flow rate adjustment is usually achieved by changing the powder carrying capacity of the fluidization gas, such as changing the flow rate of fluidization gas. It is generally not necessary to change the opening of the throttling channel [4], so the adjustment method is relatively simple. The movement state of particles in the airflow is mainly affected by its own gravity, pressure gradient force and gas flow drag force [13,14]. When the pressure drop of the throttle channel is low, the ability of fluidization gas to carry powder is weak, so there is an upper limit for the powder mass flow rate at non-choked powder supply mode. Due to the lack of understanding of this upper limit, the existing researches use non-choked powder supply mode to adjust the flow from small to large, and the large flow is usually lower than the design value [15]. Therefore, determining the upper limit for the powder mass flow rate conveyed by the non-choked powder supply mode is very important for thrust regulation of powder rocket engine. For the gas-solid two-phase flow at the throttling channel, it can be accurately described by establishing the momentum equation of the particles in the gas flow [16,17], but the solution process of this method is more complicated. Since the gas-solid two-phase flow also has some compressibility like the pure gas, it can be described simply by referring to the aerodynamic method.

For choked powder supply mode, the pressure drop of the throttle channel is relatively large, so a large flow peak will appear during the start-up process of the powder supply system [18,19]. Shen Huijun [10] believes that if the powder tank is not full, the flow peak can be eliminated. However, this method will not only reduce the powder filling rate of the tank, but also increase the response time. When the downstream pressure of the throttle channel is high, the upstream pressure required will be high too, and the pressure of the gas source will be very high finally. In this case, the gas cylinder must be very thick, which is not conducive to the lightning of the powder engine. The fluctuation of powder pneumatic conveying will have a certain influence on the pressure of the combustion chamber. The analysis of the effective fluctuation frequency of the powder supply system is helpful to analyze the oscillation characteristics of the combustion chamber.

Similar to the pure gas phase, the gas-solid two-phase flow at the throttle channel needs to meet the condition of critical pressure ratio to reach the choked state [20,21]. In order to determine the critical pressure ratio, the commonly used research method is to obtain the curve of mass flow versus stagnation pressure through a large number of experiments. In the non-choked state, the curve of mass flow versus stagnation pressure is parabolic-like, while in the choked state, the mass flow rate changes linearly with the stagnant pressure, so the critical pressure ratio can be determined by the tangent point of the straight part and the curve part. The research results show that the thermal conductivity of particles has a great impact on the critical pressure ratio of gas-solid two-phase flow [12]. This is because the gas-solid two-phase flow in the throttling channel is a two-phase non-equilibrium flow. The temperature of the solid phase cannot be changed synchronously with the gas phase (i.e. thermal relaxation), so the heat transfer rate of the two phases is affected by the thermal conductivity of the solid phase. However, the powder propellant is usually not a single-component substance, and its thermal conductivity is difficult to obtain. At the same time, the downstream pressure of the throttle channel is usually atmospheric pressure in the existing experimental researches. While in powder engines, the downstream pressure of the throttle channel is the pressure of combustion chamber [22], so it is difficult to learn from the existing theoretical results and experimental methods. It is necessary to conduct separate experimental researches on powder propellants.

In this work, a semi-empirical mass flow rate model of gas-solid two-phase at non-choked mode was established. Based on the model, the flow adjustment methods and the upper limit of powder mass flow rate at non-choked mode are obtained. At the same time, a powder supply system and a pressure simulator are set up. By changing the pressure of the pressure simulator, the choking and non-choking powder supply experiments can be carried out to further study the transition from choked flow to non-choked flow, flow adjustment characteristics and the influence of the initial pressure on the starting characteristics.

2. Approach

2.1. Experimental system

The schematic diagram of the powder supply experimental system is shown in Fig. 1. The system consists of gas source, powder supply system, and acquisition control system, pressure simulator. The gas source can provide gas to the powder supply system and pressure simulator.

The detailed composition of the powder supply system is shown in Fig. 2. The gas flowing into the powder supply system is divided into two parts, one part (i.e. actuation gas) enters the actuation chamber, and the other part (i.e. fluidization gas) enters the fluidization chamber. Actuation gas flow and fluidization gas flow can be regulated by changing the opening of the gas adjustable restrictive valve. In fact, when the powder storage tank is not filled with powder fuel, the placement of the powder storage tank will affect the fluidization profile of the powder fuel in the fluidization chamber under the influence of gravity. In order to reduce the influence of the powder storage tank placement method on the powder fluidization, the internal space of the storage tank is completely filled with powder fuel. Therefore, regardless of the placement method (vertical or horizontal) of the powder storage tank, the powder filling state in the fluidization chamber is almost the same before the experiment. The research of the silo in the industry shows that the fluidization chamber filled with powder will not affect the powder transportation. In view of the small particle size and gravity of the powder, a porous wall is used to ensure the uniformity of powder fluidization.

The mass flow rate of actuation gas ($\dot{m}_a$) required during the operation of the powder supply system can be expressed as equation (1). Where ρ_{gac} represents the gas density in the actuation chamber, and A_{tank} represents the cross-sectional area of the tank.

$$\dot{m}_a = \rho_{gac} A_{tank} \frac{ds}{dt} \tag{1}$$

The powder mass flow rate ($\dot{m}_p$) can be calculated indirectly by the displacement of piston [6], as in equation (2). Where ρ_{bulk} is the powder bulk density in the tank.

$$\dot{m}_p = \rho_{bulk} A_{tank} \frac{ds}{dt} \tag{2}$$

It can be seen from equation (1) and (2) that the speed of the piston can be changed by adjusting the actuation gas flow, so as to achieve the adjustment of the powder mass flow rate. However, in order to ensure that the powder propellant in the fluidization chamber can flow out smoothly, it is also necessary to change the fluidization gas flow and the opening of powder adjustable restrictive valve.

The acquisition system can measure the piston displacement (s), pressure of actuation chamber (p_{ac}), pressure of fluidization chamber (p_{fc}), pressure of pressure simulator (p_{ps}), upstream pressure (p_{ute}) and downstream pressure (p_{dte}) of powder adjustable restrictive valve. Sampling frequency is 5000 Hz. The accuracy of the displacement sensor (WPS-1500-V) and the pressure sensor (DaCY420) are ±0.1%, ±0.25% respectively. The control system is used to control the starting, closing and adjusting of the experimental system.

In a powder engine (ramjet or rocket engine), the powder supply system is isolated from the combustion chamber. Only the pressure of the combustion chamber may affect the operation of the powder supply system. Therefore, a pressure simulator can be used to simulate the

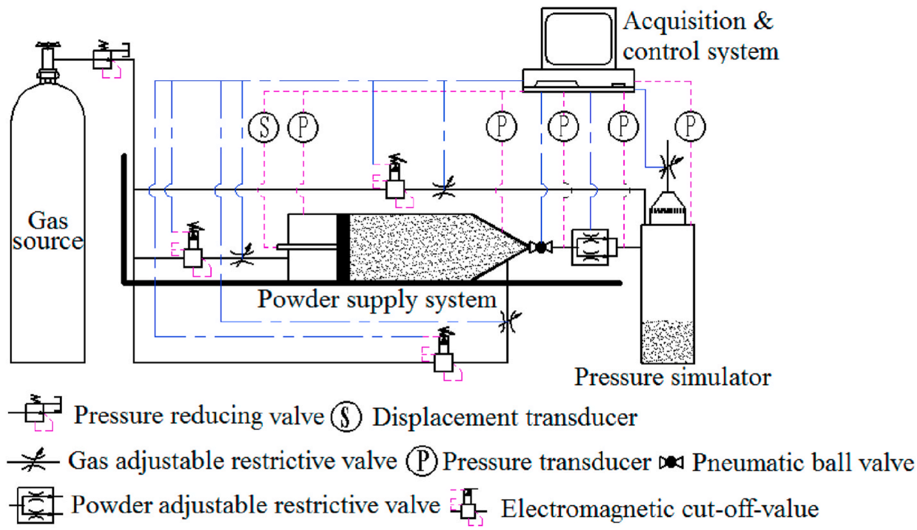

Fig. 1. Schematic diagram of the powder supply experimental system.

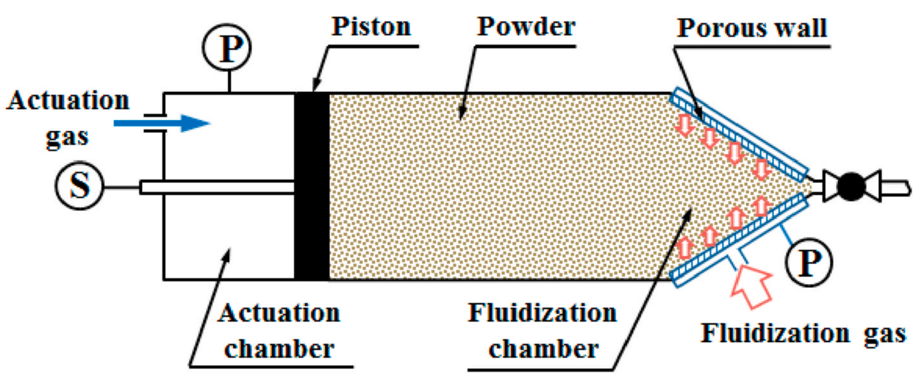

Fig. 2. Powder supply system.

pressure of the combustion chamber. Since the pressure of the cold simulation experiment is consistent with the engine experiment, the experimental results obtained by the cold calibration can be applied to the actual powder engine. The working principle of pressure simulator is to inflate the pressure simulator in advance until its internal pressure reaches the simulated pressure. In order to ensure the stability of the internal pressure of the pressure simulator, the mass flow rate of fluidization gas ($\dot{m}_f$) needs to be equal to the mass flow rate of gas flowing out from the pressure simulator, which can be achieved by adjusting the opening of the gas adjustable restrictive valve on the outlet line of the pressure simulator.

2.2. Powder supply methods

2.2.1. Choked powder supply mode

The choked powder supply mode means that during the operation of the powder supply system, there is a large pressure drop between the fluidization chamber and the combustion chamber which are the upstream and downstream of the throttle channel, and the critical pressure ratio is satisfied. If the gas and powder are mixed uniformly, the mass flow rate [9] at choked state in this paper can be expressed as follow:

$$\dot{m}_{\mathrm{mix}} = K\frac{p_{\mathrm{fc}}A}{\sqrt{R_{\mathrm{mix}}T}} \tag{3}$$

$$R_{\mathrm{mix}} = \frac{R_{\mathrm{g}}(1-\varphi)}{1-\varepsilon_p} \tag{4}$$

$$\varphi = \frac{n}{1+n} \tag{5}$$

$$\varepsilon_{\mathrm{p}} = \frac{n}{n+\rho_{\mathrm{p}}/\rho_{\mathrm{g}}} \tag{6}$$

$$m = \frac{\rho_{\mathrm{p}}}{\rho_{\mathrm{g}}} \tag{7}$$

$$n = \frac{\dot{m}_{\mathrm{p}}}{\dot{m}_{\mathrm{g}}} \tag{8}$$

where $\dot{m}_{\mathrm{mix}}$ is the mass flow rate of mixture, p_{fc} is the pressure of fluidization chamber, A is the area of throttle channel, R_{mix} is the mixing constant of two-phase, T is the temperature of two-phase flow, K is a constant, related to the specific heat ratio of the two-phase mixture, φ is the mass fraction of particle, ε_p is the volume fraction of particle.

m is the density ratio of powder to fluidization gas, n is mass ratio of powder to fluidization gas.

Equation (3) shows that the main parameters affecting the mass flow rate of two-phase flow at choked state arep_{fc}, A, n. The pressure of fluidization chamber (p_{fc}) can be increased by increasing the fluidization gas flow, thereby increasing the powder mass flow rate. However, it is difficult to reduce the powder mass flow rate by reducing the pressure of the fluidization chamber. Because this method needs to discharge a certain amount of gas in the fluidization chamber, and will bring out a certain amount of powder. The mass flow rate of gas-solid two-phase flow is proportional to the throttle channel area, so the powder mass flow rate can be easily adjusted by changing the area of the throttle channel. The method of changing the mass ratio of powder to gas can adjust the powder mass flow rate, but it can also cause the pressure of the fluidization chamber to change.

In the choked powder supply experiments, the fluidization gas has two functions. On the one hand, it is used to fluidize and transport the powder, and on the other hand, it is to maintain the pressure of the fluidization chamber to ensure that the fluidization chamber pressure and back pressure meet the critical pressure ratio. In this research, according to the method of maintaining the pressure of the fluidization chamber, choked powder supply modes can be divided into two modes (mode A and mode B). Mode A means that the actuation chamber and fluidization chamber of the powder supply system are directly connected to the gas source. The fluidization gas flow rate is determined by the gas output of the throttle channel. Mode B means that the amount of fluidization gas and actuation gas can be controlled by a gas flow regulating valve. In mode A, the powder flow adjustment can be realized by only changing the area of the throttle channel, but the controllability is poor. In mode B, the throttle channel area, the mass flow rate of actuation gas and fluidization gas must be changed at the same time, so it more complicated, but the controllability is better.

2.2.2. Non-choked powder supply mode

The non-choked powder supply mode (mode C) means that during the operation of the powder supply system, the pressure drop between the fluidization chamber and the combustion chamber is low, and the gas-solid two-phase flow at the throttle channel is in a non-choked state. If the gas-solid two-phase flow is mixed uniformly and balanced, the density of two-phase flow can be calculated by equilibrium flow equation of state, as follow:

$$\rho_{\text{mix}} = \frac{p_{\text{fc}}}{R_{\text{mix}} T} \tag{9}$$

Substituting equations (4)–(6) into equation (9)

$$\rho_{\text{mix}} = \frac{p_{\text{fc}}}{R_g} \frac{mn}{m+n} \tag{10}$$

According to the Bernoulli equation, the mass flow rate of the gas-solid two-phase flow at the throttle channel can be expressed as Equation (11).

$$m_{\text{mix}} = C_d A \sqrt{2\rho_{\text{mix}} \Delta p} \tag{11}$$

C_d is the flow coefficient of the throttle channel. Combining Equation (10) and Equation (12)

$$m_{\text{mix}} = C_d A \sqrt{2 \frac{p_{\text{fc}}}{R_g} \frac{mn}{m+n} \Delta p} \tag{12}$$

Equation (12) shows that the main parameters affecting the mass flow rate of gas-solid two-phase at non-choked state are p_{fc}, A, n, Δp. Similar to the choked powder supply mode, mode C is also difficult to achieve powder mass flow rate from large to small through the adjustment of p_{fc} and Δp. In mode C, changing the area of the throttle channel is still a useful way to adjust the powder mass flow rate, but this method usually requires a powder adjustable restrictive valve. The pressure of fluidization chamber is affected easily by the downstream pressure of the throttle channel in mode C [1], so changing the area of the throttle channel has no obvious advantage over the choked powder supply mode. It's easy to find from equation (12) that the mass flow rate of two-phase flow increases with A, p_{fc} and Δp, but the effect of n on the two-phase mass flow rate needs to be further discussed.

2.3. Experimental conditions

In order to ensure the ignition and combustion performance of the powder fuel, the particle size of the powder fuel used in the powder engine is usually less than 100 μm [1]. At the same time, the powder fuel should have good fluidization and the particle size should not be too small. Otherwise, the powder fuel will agglomerate obviously under the influence of van der Waals force or be compacted under the influence of flight overload force and piston squeezing force, which is difficult to fluidize and transport. The powder fuel used in the powder engine generally has good fluidization and transportation performance, so the pneumatic conveying performance of the powder fuel is mainly related to the gas pressure and the cross-sectional area of the pipeline [23], but not to the type of particles. Therefore, aluminum powder with a nominal particle size of 20 μm is used as the experimental powder sample (Shanghai st-nano science and technology Co., Ltd), which has good fluidization and transportation performance [6]. The natural bulk density of the powder sample is 1320 kg/m^3。 The laser particle size analysis result of the powder sample is shown in Fig. 3, which shows the average diameter the aluminum powder is about 20 μm。 In Fig. 3, D [3,4] and D [2,3] represent the volume average diameter and surface area average diameter of the particles, respectively. The greater the difference between them, the wider the particle size distribution. In addition, D(0.1) means that the volume fraction of particles smaller than this value is 10%, and the meaning of D(0.5) and D(0.9) is the same as D (0.1). Therefore, the value of D(0.5) represents the median particle size of the powder sample. Fig. 4 shows the SEM image of the aluminum powder, it can be seen that the aluminum particles have a regular and spherical shape. In this research, the gas source is air. The experimental conditions are summarized in Table 1.

For choked powder supply mode A, Test 1#, test 2# and test 3# were conducted to investigate the effects of diameter of throttle channel on working process, and test 4# is conducted to investigate the flow adjustment performance.

For choked powder supply mode B, test 5# and test 6# were conducted to investigate the effect of the initial pressure of fluidization chamber on starting characteristic. In addition, the effects of variable downstream pressure of the powder adjustable restrictive are studied by continually inflating the pressure simulator. When the pressure of the pressure simulator affects the pressure of fluidization chamber, it indicates that the gas-solid two-phase flow at the powder adjustable restrictive valve has just reached the critical point of choked flow. Before investigating the flow adjustment performance of choked powder supply mode B combined with mode C, this study first calibrated the parameters for small flow conditions (test 7#) and large flow conditions (test 8#). Because the powder mass flow rate of test 7# is small, the downstream pressure of the powder adjustable restrictive valve is also generally low, so the choked powder supply mode B can be used for small flow conditions. Since the powder mass flow rate at the choked mode is not affected by the downstream pressure of the powder adjustable restrictive

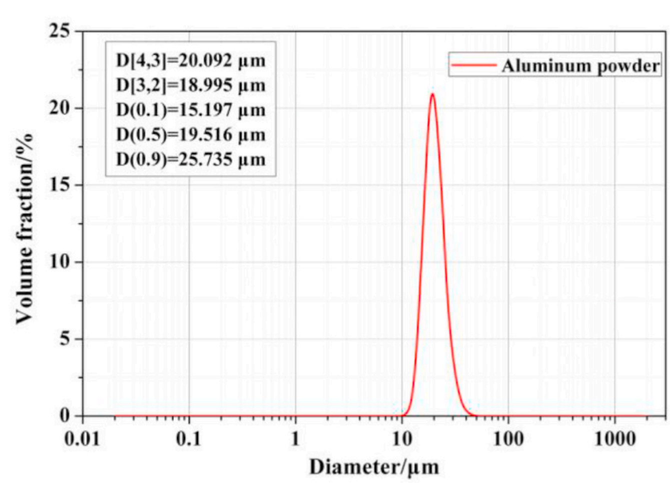

Fig. 3. Particle size distribution of aluminum powder sample.

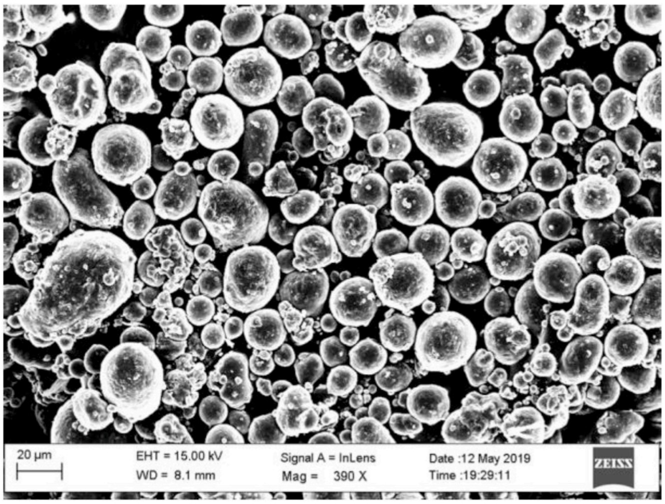

Fig. 4. SEM image of the aluminum powder.

Table 1
Experimental conditions.

Test No.	$p_{fc\_initial}$ (MPa)	$\dot{m}_f$(g/s)	d_{te}(mm)	Powder supply mode
1#	3		0.85	Mode A
2#	3		1.5	Mode A
3#	3		3.5	Mode A
4#	3		1.5 → 3.5→1.5	Mode A
5#	1.3	3.5	1.5	Mode B
6#	1.1	3.5	1.5	Mode B
7#	2	3	1.2	Mode B
8#	2	4.8	2	Mode C
9#	2	3 → 4.8→3	1.2 → 2→1.2	Mode B→Mode C→Mode B

valve, the pressure of the outside in the test 7# is set to the atmospheric pressure. However, the downstream pressure of the powder adjustable restrictive valve is generally higher under the large flow condition. In test 8#, the pressure of the pressure simulator is higher (1.75 MPa). In order to ensure the gas-solid two-phase flow was choked at the powder adjustable restrictive valve, the pressure of the fluidization chamber needed to reach more than 3.5 MPa, and the pressure of the gas source needed to be higher. Thus, the non-choked powder supply mode is used for test 8#. Based on the test 7# and test 8#, test 9# was carried out to study the adjustment characteristics of powder supply system that the powder mass flow rate is adjusted from small to large, and then to small.

3. Results and discussions

3.1. Starting characteristic

During the starting stage of the powder engine, if the mass flow rate of the powder fuel delivered by the powder supply system is too small, the energy generated by the fuel combustion may not be enough to ensure the successful ignition of the subsequent powder fuel. However, if the powder fuel flow rate is too large, the ignition may fail due to insufficient ignition energy. Therefore, the starting stage of the powder supply system is preferably a smooth process. The working process of the powder supply system under different powder supply modes is shown in Fig. 5, Fig. 6 and Fig. 7. The experimental results show that during starting stage of the choked powder supply experiments (mode A and mode B), the pressure curves of the actuation chamber and the fluidization chamber drop rapidly, and the piston displacement curves suddenly rise. It indicates that there is a flow peak in the choked powder supply experiment. However, the pressure curves of the actuation

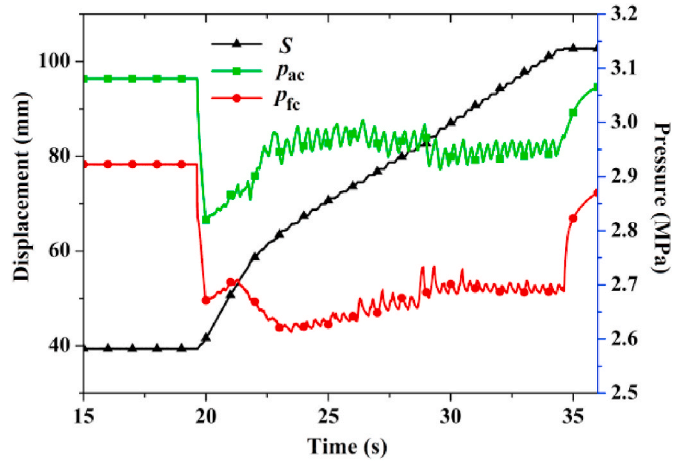

Fig. 5. The working process of the choked powder supply experiment in mode A (test 1#).

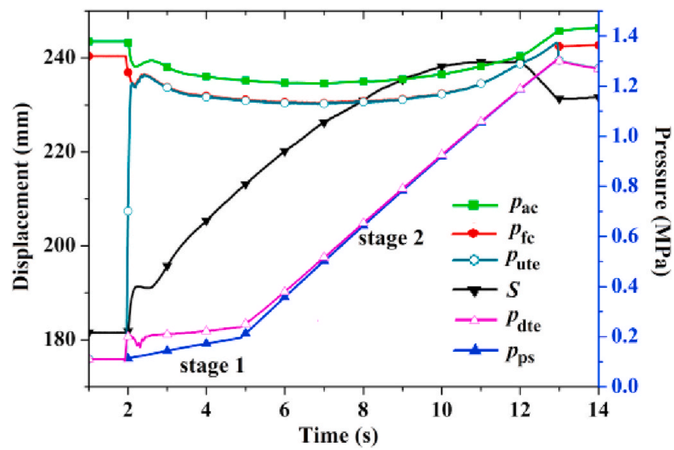

Fig. 6. The working process of the choked powder supply experiment in mode B (test 5#).

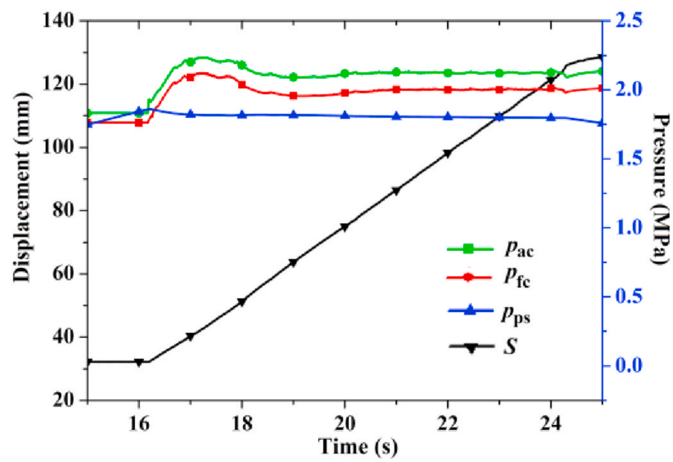

Fig. 7. The working process of the non-choked powder supply experiment in mode C (test 8#).

chamber and the fluidization chamber rise slowly, and the piston displacement curve is smooth. In the choked powder supply experiment, the initial pressures of the actuation chamber and the fluidization chamber are higher than the working pressure in the stable stage, so the gas-solid two-phase flow formed in the fluidization chamber can flow out of the powder storage tank at a faster speed. Therefore, the powder supply system will have a larger flow peak during the starting stage. In the non-choked powder supply experiment (mode C), the initial pressure of the actuation chamber and the fluidization chamber is lower than the working pressure in the stable stage, and speed of the two-phase flow flows out of the powder storage tank is slow, so there is no start-up flow peak.

In mode A, the fluidization chamber is directly connected to the gas source. Only when the fluidization chamber pressure is lower than pressure of the gas source, the gas will enter the fluidization chamber, so the fluidization chamber pressure in the stable working stage must be less than the initial pressure. Therefore, the powder starting flow peak is unavoidable in mode A [24]. In mode B, the mass flow rate of fluidization gas can be actively controlled, and the initial pressure of fluidization chamber can be lower than the working pressure in the stable stage. In the test 6# shown in Fig. 8, the initial pressure of the actuation chamber and the fluidization chamber is lower than the pressure in the starting stage, and the piston displacement curve grows very smoothly. Therefore, the initial flow peak can be weaken by setting the initial pressure value in mode B.

3.2. Stability and repeatability

3.2.1. Stability of operation process

Figs. 6, Figs. 7 and 8 show that the working process of powder supply system is more stable in mode B and mode C. However, there are obvious fluctuations in mode A. The working process of the powder supply system under different throttle channel diameter in mode A is shown in Fig. 9, and the experimental results show that the fluctuation phenomenon in mode A has nothing to do with the area of the throttle channel. Under different pressures, the working process of powder supply system in mode A also fluctuates [24].

The experimental results show that the fluctuation originates from the starting stage of the powder supply system. Since the powder flow rate in the starting stage is greater than the flow rate in the stable working phase, the powder will be clogged at the throttling channel, which will reduce the gas output of the powder storage tank and increase the pressure of the fluidization chamber. The increase in the pressure of the fluidization chamber will reduce the moving speed of the piston, which will cause the pressure in the actuation chamber to rise. Therefore, during the working process of the powder supply system, the pressure of the actuation chamber lags behind the pressure of the fluidization chamber, as shown in Fig. 10. After the pressure of the fluidization chamber rises, the pressure difference between the fluidization chamber and the outside will increase, and the powder clogged in the throttle channel will be blown off, so the pressure of the fluidization chamber will drop again. In mode A, the mass flow rate of fluidization gas is determined by the output of the powder supply system, so the clogging phenomenon at the throttle channel causes the pressure of the fluidization chamber to fluctuate with the fluctuation of the fluidization gas flow.

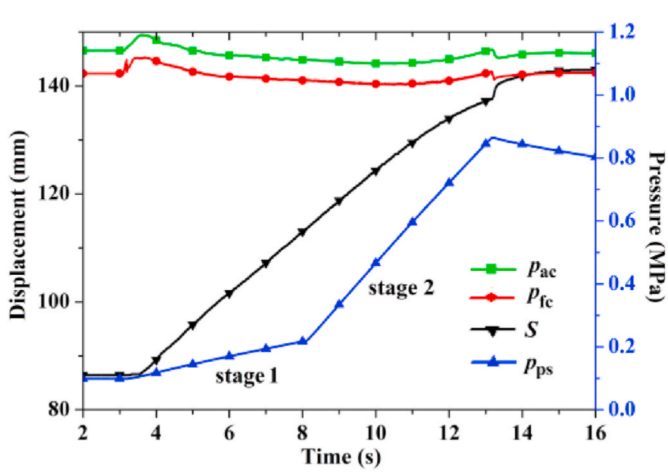

Fig. 8. The working process of the improved choked powder supply experiment in mode B (test 6#).

The fluctuation frequency and amplitude of the system under different throttle channel diameter through the Fourier analysis of the actuation chamber pressure are shown in Fig. 11. With the increase of the throttle channel diameter, the frequency of the actuation chamber pressure increases almost linearly, while the amplitude decreases exponentially. It can be inferred that if the diameter of throttle channel continues to increase, the fluctuation frequency will continue to increase, but the amplitude is very small, the impact on the powder flow of the powder supply system is almost negligible, so the powder supply system may have a maximum effective frequency. When the diameter of throttle channel is small, the powder clogged at the throttle channel is serious. Therefore, it takes longer time for the fluidization chamber pressure to form a larger pressure difference with the outside to blow the clogged powder out of the throttle channel, so the fluctuation amplitude is larger and the fluctuation frequency is lower. When throttle channel diameter is large, the powder flow smoothly, so the fluctuation amplitude is small and the fluctuation frequency is high.

It can also be seen from the experimental results that the average piston velocity obtained by differential displacement and the pressure drop of the fluidization chamber at stable stage increase with the increase of the throttle channel area, as shown in Fig. 12. Since the powder mass flow rate is proportional to the speed of piston, the powder mass flow rate also increases with the increase of the throttle channel area.

3.2.2. Repeatability of powder supply system

Due to the clogging phenomenon at the throttle channel in mode A, the repeatability of this mode must be verified. The repetitive test results of test 1#, test 2#, test 6# and test 8# are shown in Figs. 13-16 respectively. For the convenience of comparison, the results of the first test and the repetitive test are put together in one figure and the starting point of the displacement is unified. In mode A, when the diameter of throttle channel is small (0.85 mm), the repeatability of the displacement curve is poor. However, when the diameter of throttle channel is large (1.5 mm), the slopes of the two displacement curves are almost the same, with good repeatability. When the area of the throttle channel is small, the clogging phenomenon of the gas-solid two-phase flow at the throttle channel is more serious, and it will affect the fluidization state of the powder in the powder storage tank, so the powder mass flow rate will fluctuate. However, when the area of the throttling channel is large, the slight clogging phenomenon has little effect on the fluidization state of the powder in the powder storage tank, so the repeatability of the powder flow is better. Since there are no flow peaks and fluctuations in mode B and mode C, the fluidization state of the powder in the powder storage tank is relatively stable, so the repeatability is better.

3.3. Adjustment characteristics of powder mass flow rate

Based on the calibration results of Test 2# and Test 3#, the flow adjustment experiment in mode A is carried out, and the experiment result is shown in Fig. 17. The average piston speeds of the three stages are 13.1 mm/s, 11.8 mm/s and 53.5 mm/s respectively, which are similar to the calibration experiment results (Test 2# and Test 3#). In test 4#, the two flow adjustment processes are smooth, and the adjustment ratio of small flow to large flow is 4.08, which is similar to the adjustment ratio (4.53) of large flow to small flow. Therefore, choked powder supply mode A has good flow regulation performance. Fig. 17 shows that there is no flow peak during the transition from stage 2 to stage 3. This is because the stable working pressure of stage 3 is higher than the stable working pressure of stage 2.

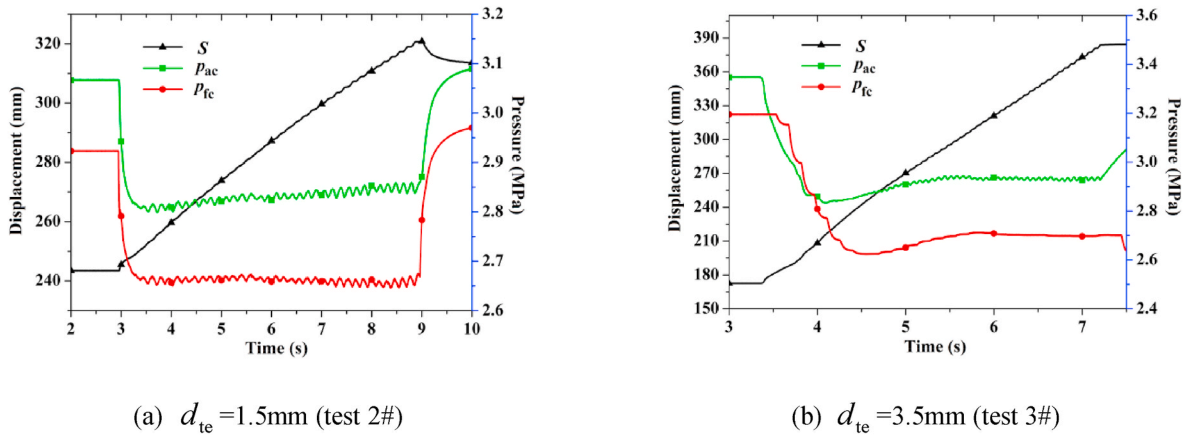

Fig. 9. Working process under different throttle channel diameter (mode A).

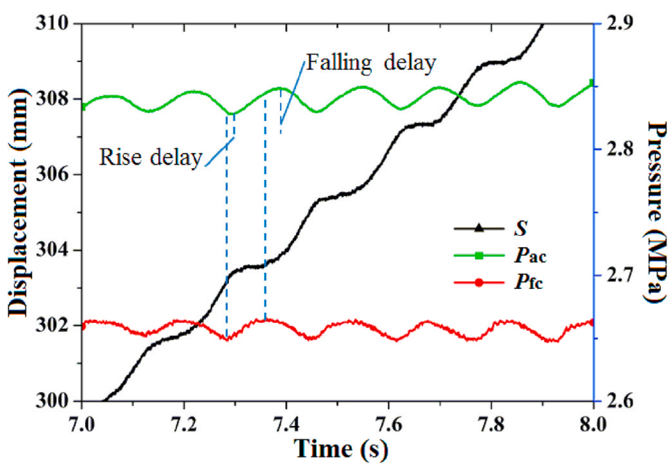

Fig. 10. Asynchronous fluctuation of displacement and pressure.

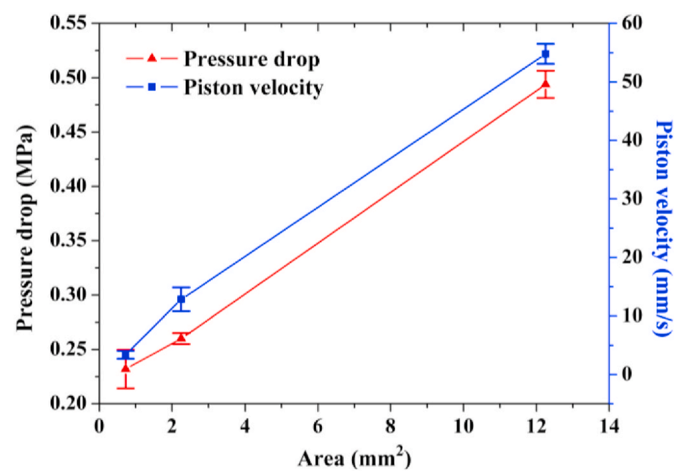

Fig. 12. The curves of mean piston velocity and pressure drop under different throttle channel area.

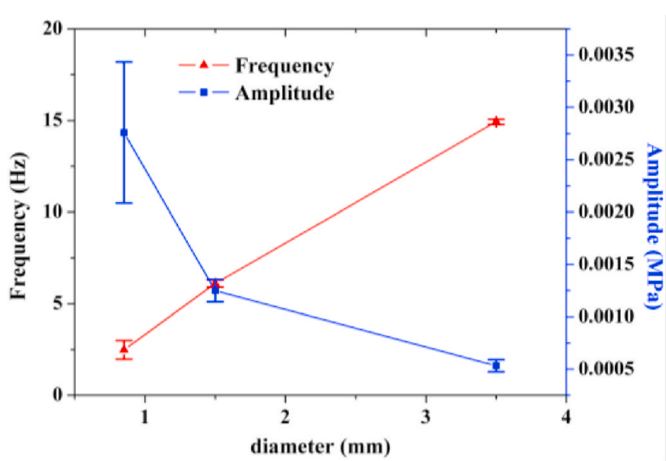

Fig. 11. The curves of fluctuation frequency and amplitude under different throttle channel diameter.

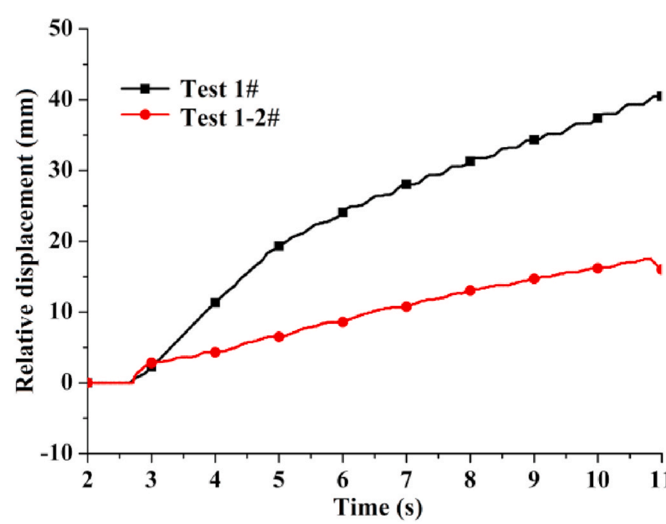

Fig. 13. Repetitive experiments of test 1# (d_{te}=0.85 mm).

In flow adjustment test 9#, powder supply mode B is adopted for small flow condition, and powder supply mode C is adopted for large flow condition. Test 7# is the calibration experiment result of small flow condition, as shown in Fig. 18. Based on the calibration results of test 7# and test 8#, the flow adjustment experiment in mode B combined with mode C is carried out, and the experiment result is shown in Fig. 19. The first stage and the third stage are the working process of small flow condition, and the designed parameters of them are the same. The second stage is the working process of large flow condition. The results show that the adjustment process from the first stage to the second stage is very smooth. The velocity of piston is adjusted from 2.96 mm/s to

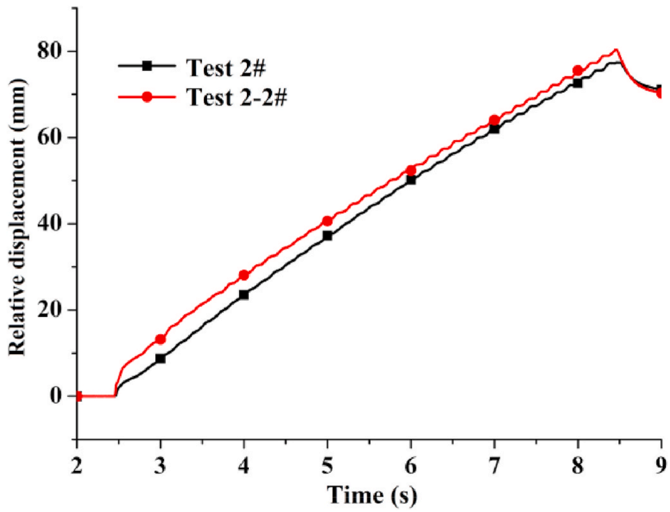

Fig. 14. Repetitive experiments of test 2# (d_{te}=1.5 mm).

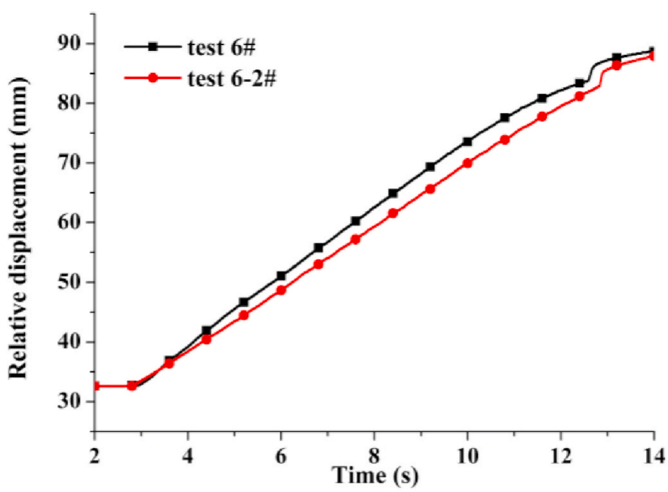

Fig. 15. Repetitive experiments of test 6#.

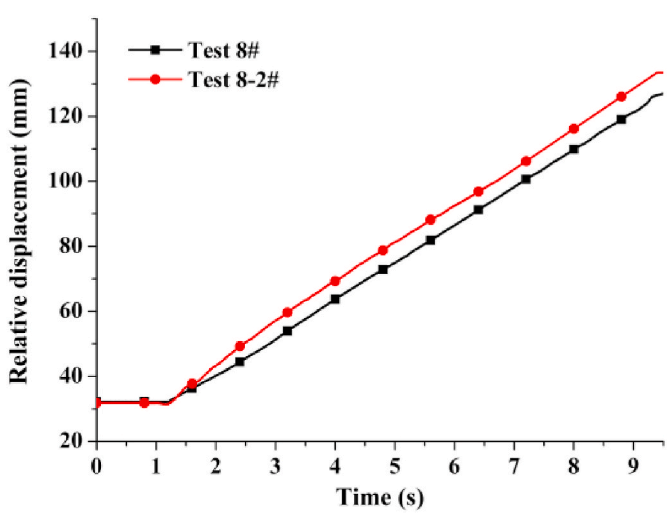

Fig. 16. Repetitive experiments of test 8#.

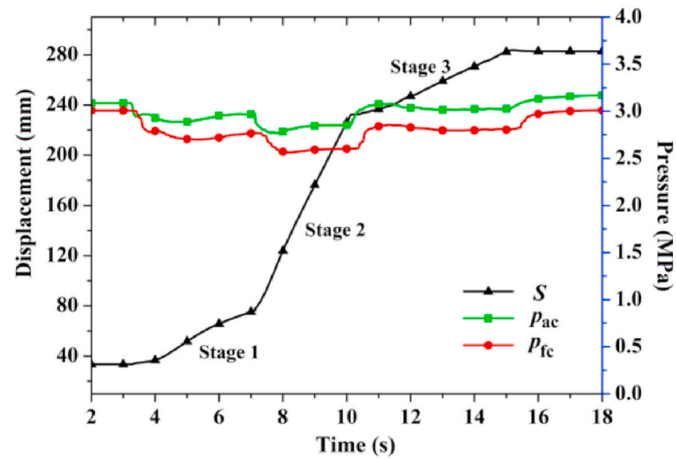

Fig. 17. Flow adjustment experiment in choked powder supply mode A (test 4#).

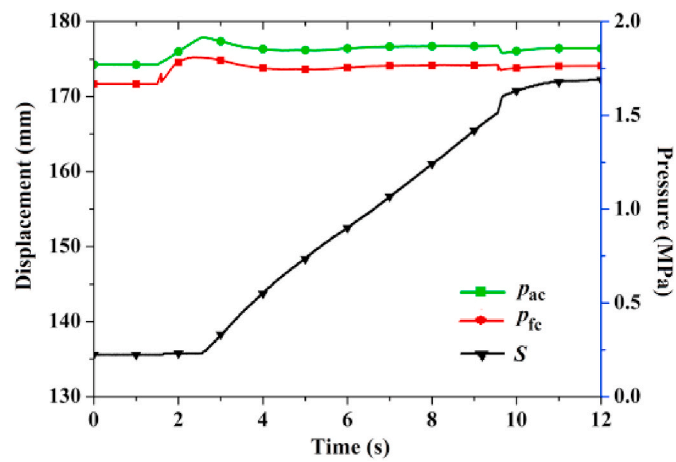

Fig. 18. The working process of the choked powder supply experiment in mode B (test 7#).

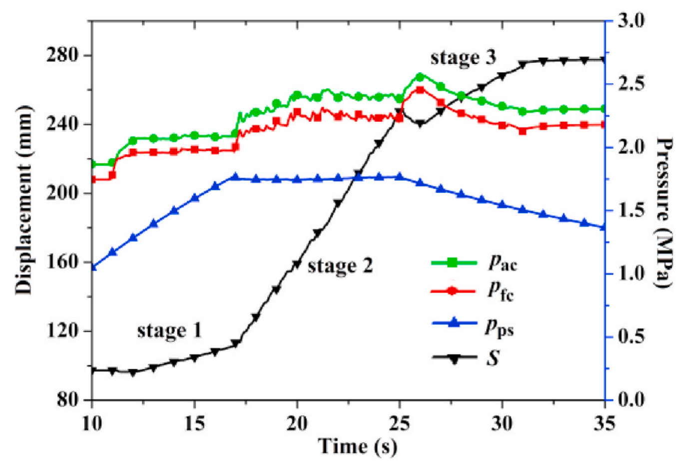

Fig. 19. Flow adjustment experiment in mode B combined with mode C (test 9#).

16.8 mm/s, and the adjustment ratio is 5.68. The average speed of the piston in the second stage is greater than the result of calibration experiment (test 8#). Before the stage 2, the powder supplied in stage 1 already exists in the pipeline, which causes the pressure drop at the throttle channel of the second stage to be greater than the design value. Thus, the powder flow rate in stage 2 is also greater than the design value. In stage 3, the pressure of actuation chamber and fluidization chamber is greater than the pressure in stage 1. Therefore, according to equation (3), the velocity of the piston (6.8 mm/s) in the third stage is greater than the velocity of the piston in the first stage. During the transition process from stage 2 to stage 3, the large powder flow in stage 2 under the effect of inertia still flow to the throttle channel of the third stage, which leads to a reduction in the area of the throttling channel in stage 3. Therefore, the pressure of the fluidization chamber rises in stage 3. And then, since the mass flow rate of the fluidization gas in stage 3 is lower than that of the stage 2, the pressure of the fluidization chamber continuously decrease. In addition to the better repeatability of the average displacement speed in stage 1, the average piston displacement speed in the other two stages is quite different from the design value, so the adjustment performance of this method is worse than that of the choked powder supply mode A.

According to the adjustment method of the powder mass flow rate mentioned above, the mass flow rate of powder can be reduced by increasing the mass flow rate of fluidization gas. Therefore, on the basis of test 8#, this study increased the mass flow rate of fluidization gas in the third stage (from 3 g/s to 6.3 g/s), and kept the mass flow rate of actuation gas unchanged. Because the mass flow rate of fluidization gas is greater than that of the second stage, it can hinder the movement of the piston and reduce its velocity, thereby achieving the purpose of reducing the powder mass flow rate. The experimental results after increasing the fluidization gas are shown in Fig. 20. At the transition stage, the velocity of the piston decreases rapidly and then gradually rises to a stable state. The pressure of fluidization chamber and the actuation chamber is stable after the transfer. In this experiment, the average velocity of the piston in the stage of small powder mass flow rate is 2.65 mm/s, which is similar to the velocity of the piston in the first stage of test 9#, indicating that increasing the mass flow rate of fluidization gas can usefully reduce the powder mass flow rate. Although the powder flow rate can be changed from large flow to small flow by adjusting the fluidization gas flow rate, additional calibration experiments are usually performed to meet the actual engine work requirements.

3.4. The flow upper limit of non-choked mode

Taking the parameters in Table 2 as an example, the influence of mass ratio of powder to fluidization gas at the non-choked powder supply mode is studied.

The mass ratio of powder to fluidization gas in Table 2 is 1. If the mass flow rate of fluidization gas is constant, n increases with the powder mass flow rate, and the result (m_{mix}) calculated by equation (12) and the sum ($\dot{m}_{\mathrm{p}} + \dot{m}_{\mathrm{g}}$) of the mass flow rate of powder and fluidization gas are shown in Fig. 21. When powder mass flow rate is constant, n decreases with the increase of mass flow rate of fluidization gas, and the result calculated by equation (12) and the sum of the mass flow rate of powder and fluidization gas are shown in Fig. 22. It can be seen from Fig. 21 that the mass flow rate of two-phase flow decreases with the decrease of n, so it can be reduced by increasing the amount of fluidization gas. However, there is a critical point that m_{mix} is equal to $\dot{m}_{\mathrm{p}} + \dot{m}_{\mathrm{g}}$. The flow coefficient ($C_{\mathrm{d}}$) used in the calculation is the maximum value (1), so the mass flow rate calculated by Equation (12) is the maximum mass flow rate under these parameters. If the sum of the mass flow rate of powder and fluidization gas exceeds this value, it indicates that the gas-solid two-phase flow will be clogged at the throttle channel. It can be seen from Fig. 22 that gas-solid two-phase mass flow rate decreases as the mass flow rate of fluidization gas increases. When the mass flow rate of fluidization gas increases to the critical point, the mass flow rate of gas-solid two-phase at throttle channel will reach the upper limit. Therefore, in order to increase the gas-solid two-phase mass flow rate, the pressure drop at the throttle channel must be increased. When the upstream and downstream pressures of the throttle channel meet the critical pressure ratio, the non-choked powder supply mode C changes to the choked powder supply mode B.

According to equation (12), Figs. 21 and 22, it can be seen that reducing n, that is, increasing the mass flow rate of fluidization gas can achieve a large reduction in powder mass flow rate. When the area of the throttle channel is constant, increasing the mass flow rate of fluidization gas makes the gas occupy more area of the throttle channel, resulting in a decrease of powder mass flow rate. In this method, the area of throttle channel is the same at the conditions of different powder mass flow rate, so no additional powder adjustable restrictive valve is needed, and the structure of the powder supply system is simpler.

Table 2
Initial calculation parameters.

parameters	Value
C_{d}	1
d_{t}	2 mm
p_{fc}	1.1 MPa
Δp	0.1 MPa
$\dot{m}_{\mathrm{p}}$	10 g/s
$\dot{m}_{\mathrm{g}}$	10 g/s

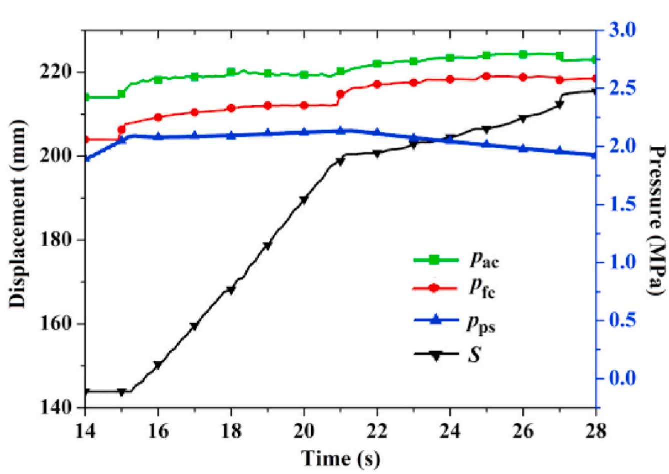

Fig. 20. Improved flow adjustment experiment in mode B combined with mode C (test 9–2#).

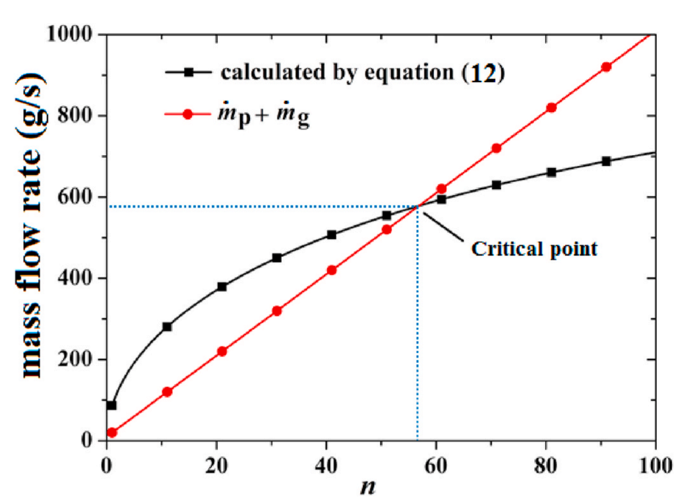

Fig. 21. Variation of two-phase mass flow rate with n (only increase the powder mass flow rate).

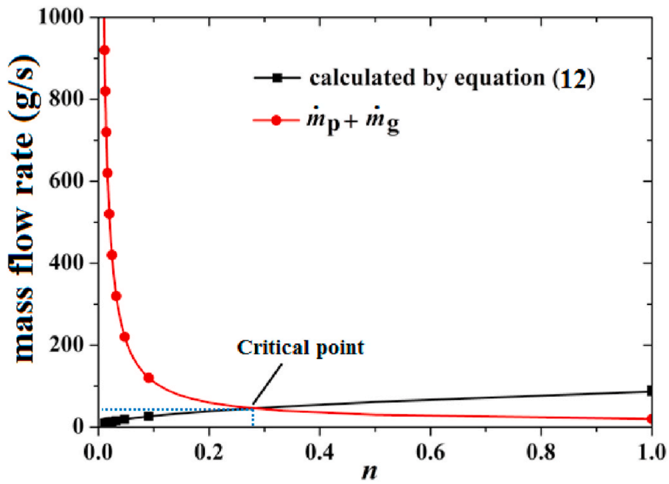

Fig. 22. Variation of two-phase mass flow rate with n (only increase the gas mass flow rate).

3.5. Pressure signal analysis and critical pressure ratio

In order to record the experimental working parameters in detail, this study set a high sampling frequency for the acquisition system, but a lot of noise signals are recorded at the same time. The noise signals will have a great impact on the identification of the critical point of the pressure of fluidization chamber. In this study, wavelet decomposition, denoising and reconstruction are performed on the pressure signal of the fluidization chamber, and then identify the critical point by the differential curve of fluidization chamber pressure.

In this study, db2 in the Daubechies series of wavelet functions [25–28] is used as the wavelet mother function to perform 8-scale wavelet analysis and wavelet reconstruction on the pressure signal of fluidization chamber in test 2# to obtain the time series of pressure signals at different scales. Since the sampling frequency of the acquisition system used in this experiment is 5000 Hz, after 8 layers of decomposition, the frequency range corresponding to the pressure signal of each scale is obtained, as shown in Table 3.

The waveform obtained by decomposing and reconstructing the pressure signal of the fluidization chamber into the wavelet is shown in Fig. 23. It can be seen from Fig. 23 that the signals of the d1-d8 layer are all noise signals, and a8 is almost the same as the original signal, indicating that the effective frequency of the powder supply system is within 20 Hz, and the researches [29,30] show that the fluctuation is mainly caused by the movement of piston.

In order to find the critical point of pressure, this study differentiates the pressure signal after wavelet denoising, and puts the result in the same graph with the pressure of the fluidization chamber, as shown in Fig. 24. There is a clear turning point in the pressure differential curve of fluidization chamber, and the pressure of the fluidization chamber is affected by the pressure rise of the pressure simulator. The velocity of the piston at the turning point can be obtained by differentiating the displacement of the piston, and the powder mass flow rate can be calculated by equation (2). Thus, the solid-gas ratio (n) of test 6# at the turning point is 2.75. According to the pressure of the fluidization chamber and the pressure simulator at the turning point, the critical pressure ratio of test 6# is 0.5512. Through the above method, the critical pressure ratio can be found to provide a basis for the choked powder supply mode.

Table 3
Frequency range of pressure signal decomposed by wavelet.

Signals of different scales	Frequency Range (Hz)	Signals of different scales	Frequency Range (Hz)
d1	2500–5000	d5	156.25–312.5
d2	1250–2500	d6	78.125–156.25
d3	625–1250	d7	39.0625–78.125
d4	312.5–625	d8	19.53125–39.0625
a8	0–19.53125		

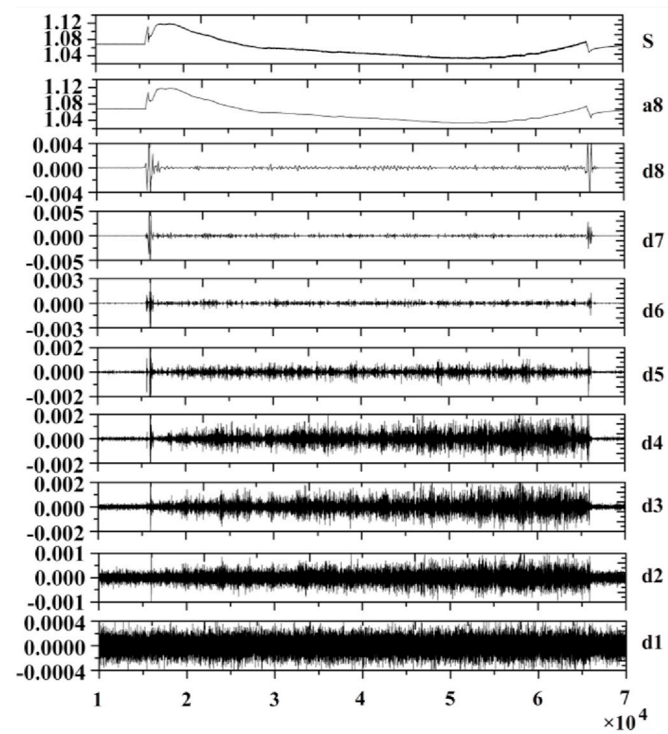

Fig. 23. Waveform obtained by decomposing and reconstructing pressure signal of fluidization chamber into wavelet.

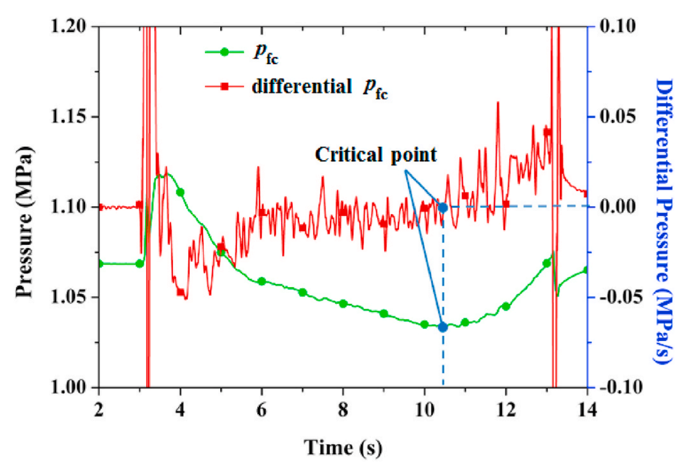

Fig. 24. Identification of critical pressure ratio.

4. Conclusions

In this paper, the characteristics of powder pneumatic conveying at choked mode and non-choked mode were studied through theoretical analysis and experiments. The main conclusions are as follows.

(1) A semi-empirical mass flow rate model of gas-solid two-phase at non-choked mode was established. The model shows that the powder mass flow rate can be adjusted by changing the pressure,

area, mass ratio of powder to gas and pressure drop. There is an upper limit of powder mass flow rate at non-choked mode.

(2) The powder supply system will fluctuate in the choked powder supply mode A. With the increase of the diameter of the throttling channel, the fluctuation frequency increases almost linearly and the fluctuation amplitude decreases exponentially, and the pressure drop of the actuation chamber lags behind the pressure of the fluidization chamber. When the diameter of the throttle channel is small, the repeatability in mode A is poor, and when the diameter of the throttle channel is large, the repeatability in mode A is better. This mode has good flow regulation performance.

(3) In the choked powder supply mode B, the starting characteristics of the powder supply system are related to the initial pressure of the fluidization chamber. When the initial pressure is higher than the pressure in the stable working stage, the powder supply system will have a flow peak, and when the initial pressure is lower than the pressure in the stable stage, the flow peak can be weakened.

(4) An experimental method and a data processing method to study the critical pressure ratio of gas-solid two-phase flow were established. The results show that the effective frequency of the powder supply system is within 20 Hz, and the critical pressure ratio of aluminum powder at the solid-gas ratio $n = 2.75$ is 0.5512.

(5) By adopting choked powder supply mode (mode B) at small flow condition and non-choked powder supply mode (mode C) at large flow condition, the adjustment of powder mass flow rate with a large back pressure variation range (0.1 MPa–1.75 MPa) is achieved, and the adjustment ratio can reach 5.68. Increasing the mass flow rate of fluidization gas, that is, reducing the mass ratio of solid to gas is easier to achieve a large reduction in powder mass flow rate.

Declaration of competing interest

The authors declare that they have no known competing financial interests or personal relationships that could have appeared to influence the work reported in this paper.

Acknowledgment

The authors acknowledge the National Natural Science Foundation of China (grant no. 51876178) and Xi'an Modern Chemistry Research Institute (Grant No. syjj38) in sponsoring this work.

References

[1] H.J. Loftus, L.N. Montanino, R.C. Bryndle, Powder rocket feasibility evaluation, in: 8th AIAA/ASE Joint Propulsion Specialist Conference, AIAA, New Orleans, Louisiana, USA, 1972, pp. 72–1162, https://doi.org/10.2514/6.1972-1162.

[2] J.P. Foote, R.J. Litchford, Powdered magnesium-carbon dioxide combustion for Mars propulsion, in: 41st AIAA/ASME/SAE/ASEE Jt. Propuls. Conf. Exhib, AIAA, Tucson, Arizona, USA, 2005, pp. 2005–4469, https://doi.org/10.2514/6.2005-4469.

[3] S. Goroshin, A.J. Higgins, M. Kamel, Powdered metals as fuel for hypersonic ramjets, in: 37th AIAA/ASME/SAE/ASEE Joint Propulsion Conference and Exhibit, AIAA, Salt Lake City, Utah, USA, 2001, pp. 2001–3919, https://doi.org/10.2514/6.2001-3919.

[4] Mike L. Meyer, Powdered aluminum and oxygen rocket propellants: subscale combustion experiments, in: 30th JANNAF Combustion Subcommittee, JANNAF, Monterey, California, USA, 1993, pp. 94–21760. https://ntrs.nasa.gov/citations/19940017287.

[5] Li Yue, Chunbo Hu, Zhe Deng, Li Chao, Haijun Sun, Yupeng Cai, Experimental study on multiple-pulse performance characteristics of ammonium perchlorate/aluminum powder rocket motor, Acta Astronaut. 133 (2017) 455–466, https://doi.org/10.1016/j.actaastro.2016.11.014.

[6] Li Chao, Chunbo Hu, Xin Xin, Li Yue, Haijun Sun, Experimental Study on the operation characteristics of aluminum powder fueled ramjet, Acta Astronaut. (2016) 74–81, https://doi.org/10.1016/j.actaastro.2016.08.032, 129.

[7] J.H. Wickman, In-situ Mars rocket and jet engines burning carbon dioxide, in: 35th AIAA/ASME/SAE/ASEE Joint Propulsion Conference and Exhibit, AIAA, Los Angeles, California, USA, 1999, pp. 99–2409, https://doi.org/10.2514/6.1999-2409.

[8] S. Goroshin, A.J. Higgins, J.H.S. Lee, Powdered magnesium-carbon dioxide propulsion concepts for Mars missions, in: 35th AIAA/ASME/SAE/ASEE Jt. Propuls. Conf. Exhib, AIAA, Los Angeles, California, USA, 1999, pp. 99–2408, https://doi.org/10.2514/6.1999-2408.

[9] Haijun Sun, Chunbo Hu, Tian Zhang, Zhe Deng, Experimental investigation on mass flow rate measurements and feeding characteristics of powder at high pressure, Appl. Therm. Eng. 102 (2016) 30–37, https://doi.org/10.1016/j.actaastro.2016.08.032.

[10] Zhixun Xia, Huijun Shen, Jianxin Hu, Bing Liu, Experimental investigation of powdered metals fuel ramjet, in: 44th AIAA/ASME/SAE/ASEE Joint Propulsion Conference & Exhibit, AIAA, Hartford, Connecticut, USA, 2008, pp. 2008–5131, https://doi.org/10.2514/6.2008-5131.

[11] T. Han, A. Levy, H. Kalman, Y. Peng, Model for dilute gas–particle flow in constant-area lance with heating and friction, Powder Technol. 112 (2000) 283–288, https://doi.org/10.1016/S0032-5910(00)00303-X.

[12] Qiang Li, Zongshu Zou, Shengming Tan, Choking phenomena of gas-powder flows at sonic velocity, Steel Research lnt 10 (2005) 669–705, https://doi.org/10.1002/srin.200506081.

[13] V.B. Betelin, N.N. Smirnov, V.F. Nikitin, V.R. Dushin, A.G. Kushnirenko, V. A. Nerchenko, Evaporation and ignition of droplets in combustion chambers modeling and simulation, Acta Astronaut. 70 (2012) 23–35, https://doi.org/10.1016/j.actaastro.2011.06.021.

[14] N.N. Smirnov, V.B. Betelin, A.G. Kushnirenko, V.F. Nikitin, V.R. Dushin, V. A. Nerchenko, Ignition of fuel sprays by shock wave mathematical modeling and numerical simulation, Acta Astronaut. 87 (2013) 14–29, https://doi.org/10.1016/j.actaastro.2013.01.023.

[15] Guanjie Wu, Quanbin Ren, Li Chao, Li Yue, Chunbo Hu, Experimental study on thrust regulation characteristics of aluminum/ammonium perchlorate powder rocket motor, J. Solid Rocket Technol. (41) (2018) 543–548 (in Chinese), http://en.cnki.com.cn/Article_en/CJFDTotal-GTHJ201805003.htm.

[16] Nickolay N. Smirnov, Valeriy F. Nikitin, Vladislav R. Dushin, Yurii G. Filippov, Valentina A. Nerchenko, Javad Khadem, Combustion onset in non-uniform dispersed mixtures, Acta Astronaut. 115 (2015) 94–101, https://doi.org/10.1016/j.actaastro.2015.04.021.

[17] Veronika V. Tyurenkova, Maria N. Smirnova, Valeriy F. Nikitin, Two-phase fuel droplet burning in weightlessness, Acta Astronaut. 176 (2020) 672–681, https://doi.org/10.1016/j.actaastro.2020.03.044.

[18] Li Chao, Chunbo Hu, Xiaofei Zhu, Jiaming Hu, Li Yue, Xu Hu, Experimental study on the thrust modulation performance of powdered magnesium and CO2 bipropellant engine[J], Acta Astronaut. 147 (2018) 403–411, https://doi.org/10.1016/j.actaastro.2018.03.029.

[19] Haijun Sun, Chunbo Hu, Xiaofei Zhu, Numerical simulation on the powder propellant pickup characteristics of feeding system at high pressure, Acta Astronaut. 139 (2017) 85–97, https://doi.org/10.1016/j.actaastro.2017.06.030.

[20] Liangju Zhao, Lijuan Gao, Qinghua Chen, Hong Gao, Danling Zeng, Shock wave of gas-solid flow considering the two-phase sound velocity, in: ASME 2005 International Mechanical Engineering Congress and Exposition, ASME, Orlando, Florida, USA, 2005, pp. 2005–80528, https://doi.org/10.1115/IMECE2005-80528.

[21] R.K. Anand, On dynamics of imploding shock waves in a mixture of gas and dust particles, Int. J. Non Lin. Mech. 65 (2014) 88–97, https://doi.org/10.1016/j.ijnonlinmec.2014.05.001.

[22] Li Yue, Chunbo Hu, Xiaofei Zhu, Experimental study on combustion characteristics of magnesium and carbon dioxide in powder rocket environment, Acta Astronaut. 155 (2019) 334–349, https://doi.org/10.1016/j.actaastro.2018.11.006.

[23] Liang Cai, John R. Grace, Shen Liu, Gaoyang Yuan, Xiaoping Chen, Zhao Changsui, Experimental investigation of pressure letdown flow characteristics in dense-phase pneumatic conveying at high pressure, Powder Technol. 277 (2015) 171–180, https://doi.org/10.1016/j.powtec.2015.03.002.

[24] Haijun Sun, Chunbo Hu, Tian Zhang, Zhe Deng, Experimental investigation on mass flow rate measurements and feeding characteristics of powder at high pressure, Appl. Therm. Eng. 102 (2016) 30–37, https://doi.org/10.1016/j.applthermaleng.2016.03.142.

[25] Li Hui, Application of wavelet multi-resolution analysis to pressure fluctuations of gas-solid two-phase flow in a horizontal pipe, Powder Technol. 125 (2002) 61–73, https://doi.org/10.1016/S0032-5910(02)00012-8.

[26] Kenneth C. Williams, Mark G. Jones, Ahmed A. Cenna, Characterization of the gas pulse frequency, amplitude and velocity in non-steady dense phase pneumatic conveying of powders, Particuology 6 (2008) 301–306, https://doi.org/10.1016/j.partic.2008.03.007.

[27] Feifei Fu, Chuanlong Xu, Shimin Wang, Flow characterization of high-pressure dense-phase pneumatic conveying of coal powder using multi-scale signal analysis, Particuology 36 (2018) 149–157, https://doi.org/10.1016/j.partic.2017.05.003.

[28] Y. Alkassar, V.K. Agarwal, N. Behera, M.G. Jones, R.K. Pandey, Transient characteristics of fine powder flows within fluidized dense phase pneumatic

conveying systems, Powder Technol. 343 (2019) 629–643, https://doi.org/10.1016/j.powtec.2018.11.081.
[29] Haijun Sun, Chunbo Hu, Yihua Xu, Pressure fluctuations analysis on the powder fluidization performance at different pressure, Int. J. Multiphas. Flow 116 (2019) 176–184, https://doi.org/10.1016/j.ijmultiphaseflow.2019.04.020.
[30] Shrikant V. Dhodapkar, George E. Klinzing, Pressure fluctuations in pneumatic conveying systems, Powder Technol. 74 (1993) 179–195, https://doi.org/10.1016/0032-5910(93)87010-L.